KSME International Journal, Vol. 12, No. 4, pp. 709~718, 1998

Forced Air Cooling by Using Manifold Microchannel Heat Sinks

Yong Il Kim*, Woo Chong Chun*, Jin Taek Kim*, Bock Choon Pak and Byoung Joon Baek****

(Received August 11, 1997)

A study of manifold microchannel (MMC) heat sinks for forced air cooling was performed experimentally. The manifold microchannel heat sink differs from a traditional microchannel (TMC) heat sink in that the flow length is greatly reduced to a small fraction of the total length of the heat sink. In other words, the MMC heat sink features many inlet and outlet channels, alternating at a periodic distance along the length of the microchannels while the TMC heat sink features one inlet and one outlet channels. The present study primarily focused to investigate the effects of geometrical parameters on the thermal performance of the manifold microchannel heat sinks for optimal design. Also, the thermal resistances of the MMC heat sinks were compared with those of the TMC heat sinks. Experimental results showed the thermal resistances of MMC heat sinks were affected strongly by the pumping power, the microchannel width and the manifold inlet/outlet channel width, but weakly by the microchannel thickness-width ratio and the microchannel depth coorporated with the manifold inlet/outlet channel width. However, it was found that there existed the optimum values of the latter parameters. Under the optimum condition of geometrical parameters in the present study, the thermal resistance of the MMC heat sink was approximately 35% lower than that of a TMC heat sink, which clearly demonstrated the effectiveness of using a manifold.

Key Words: Manifold Microchannel, Traditional Microchannel, Thermal Resistance, Air Cooling, Heat Sink, Optimization

1. Introduction

A traditional microchannel (TMC) heat sink, as fiystly proposed by Tuckerman and Pease (1981), was seen as a means of cooling integrated circuits using water as the coolant. The TMC heat sink features one inlet and outlet channel, each located at the opposite ends of the chip length, as shown in Fig. 1. While providing very high cooling capabilities, two design constraints were evident :

1. High pressure drop was required due to the combination of channel width and flow rate. This was necessary to minimize the thermal resistance.

2. Significant temperature difference within the heat source between inlet and outlet was imposed. This was due to the developing thermal boundary layer in the channels and increase in the fluid temperature along the channel length.

1.1 Motivation

In an application in which microchannels can be directly attached to inlet and outlet channels, in which a high pressure drop is acceptable, and in which high temperature variation within the heat source is acceptable or is minimized by the use of a highly conductive heat spreader, the TMC heat sink can be used. Using microchannels to cool the multichip modules may require significant modification of the microchannel concept. Chips are spaced close together, and will most likely be connected to the substrate by solder

* Dept. of Mechanical Engineering, Graduate School, Chonbuk National University

** Division of Mechanical Engineering, Chonbuk National University, Chonju, Chonbuk 561-756, Korea

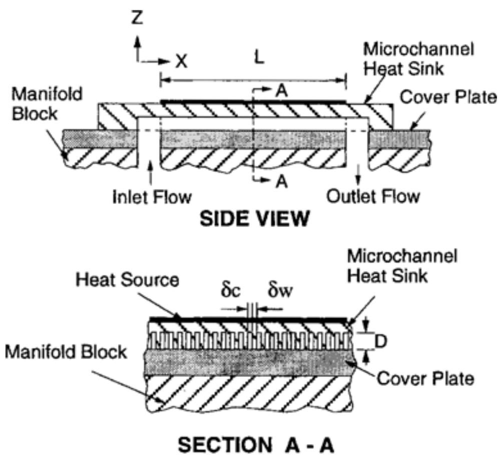

Fig. 1 Schematic view of a traditional microchannel (TMC) heat sink.

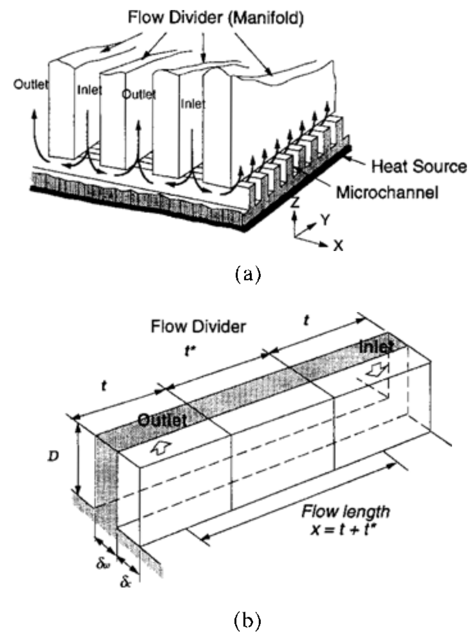

Fig. 2 Cutaway view of a manifold microchannel (MMC) heat sink.

bump arrays. The solder bump interconnection places the chips in an orientation favorable to microchannel cooling, with the (electrically active) circuitry facing the substrate and the (electrically) inactive side with the microchannels facing away. Such packaging imposes several constraints on the cooling technology :

1. The microchannels must be supplied with fluid inlet and outlet channels which require very little area in the X–Y plane of the chips and the substrate. Connection should be made as much as possible in the Z-axis (normal to the chip surface).

2. Force acting on the solder bumps may limit the allowable pressure drop through the microchannels. Additionally, a traditional microchannel exerts the wall shear in one direction, opposite to the flow. Significant differences in compressive force within the solder bump array may not be permissible.

The manifold microchannel (MMC) heat sink has been shown by Harpole and Eninger (1991) and more recently by Pak et al. (1995) to be an effective way of reducing temperaure variations within the heat source and pressure drops at a fixed volume flow rate. In view of the packaging constraints imposed by the multichip modules, it may not be possible to make a rigid, leakproof connection between the manifold and the microchannels. Reworkability may also require a separable connection. A manifold held in place by the compressive force could be used to provide fluid to the microchannels. The compressive force should be slightly greater than the resistance caused by the pressure drop through the microchannels. Such a device could tolerate differences in thermal expansion due to nonuniform heating, mismatch in coefficients of thermal expansion, transient heating or cooling, etc. Additionally, the shear forces acting on each manifold channel are balanced by the adjacent channel, so that no net shear force is applied to the solder bump array.

Figure 2 shows the configuration of the manifold microchannel heat sink used in the present study. The MMC heat sink features many inlet and outlet channels, alternating at a periodic distance along the length of the microchannels. As shown in Fig. 2(a), the flow enters the microchannels from the manifold inlet channel, splits and flows through the microchannels, then exits to the manifold outlet channel. This pattern is repeated along the direction perpendicular to the microchannel. Figure 2(b) presents a unit cell of flow domain bounded by the centerlines of the manifold inlet and outlet channels and by those of

the microchannels and heat sink walls.

The objective of the present study is to investigate the geometrical parameters such as the microchannel width and depth, the thickness-width ratio and the manifold inlet/outlet width on the performance of a manifold microchannel heat sink for optimal design. The thermal performances of the MMC heat sinks are also compared with those of the TMC heat sinks in order to examine the effectiveness of using a manifold.

1.2 Previous work

Since the microchannel heat sink was first proposed as a means of liquid cooling by Tuckerman and Pease, their original analysis and design have been modified slightly in subsequent studies. Improvements to the original design could be achieved by turbulent flow (Phillips, 1990 ; Knight et al., 1992b), wall thicknesses thinner than channel width (Harpole, 1991 ; Pak, 1995 ; Phillips, 1990; Knight, 1992a) and by manifolding (Harpole, 1991 ; Pak, 1995). Also, since then many researchers have investigated to apply for air cooling scheme.

Goldberg (1984) investigated analytically and experimentally a new style compact forced air heat sinks. The results showed that the narrow channel heat sinks using air as a cooling fluid could keep the temperature rise of 10 W chips below 60℃ (equivalent to the thermal resistance of 6℃/W).

Schulenberg et al. (1989) investigated experimentally forced air cooling in the microchannel heat sinks. Also, a simple analytical method of predicting its thermal performance was presented. They showed that the suggested analytical model could be used for predicting the thermal performance of the microchannel heat sinks, however, Nusselts number correlations suggested in their study should be used.

Knight et al. (1991, 1992b) presented detailed analyses of both laminar and turbulent flows in microchannels. The turbulent analysis was used to predict the performance of an air-cooled heat sink. At a given pressure drop, the flow rate was much lower than predicted, resulting in a much higher thermal resistance. The experimental optimum number of heat sink fins agreed with the prediction.

Gromoll (1994) demonstrated many possible forms of the heat exchanger manufactured by the silicon etching technology, which could be used as a basic component to construct the micro-air-cooling system. It has been shown that the cooling performances per unit area of the power loss source surface were achieved that were comparable with those of the liquid cooling systems.

Yu and Xin (1994) tested and analyzed the air-cooled heat sinks with 0.2 mm thick copper fins of several lengths. They used a porous-medium model to predict the thermal resistance. At a fixed volume flow rate, measured thermal resistance was slightly higher than predicted.

Kleiner et al. (1995) investigated theoretically and experimentally high performance forced air cooling scheme which employed microchannel parallel plate-fin heat sinks and tubes to deliver the air to and optionally from the heat sink. They demonstrated its thermal performances were superior to those attainable using the open air cooled heat sinks as well as those employing silicon microcoolers.

Pak et al. (1995) tested a variety of manifold microchannel with channel widths of 57 and 113 μ. The microchannel depth and the wall thickness were varied, as well as the number of manifold channels. Generally, the measured convective thermal resistance was lower than predicted, with the dependence on flow rate considerably stronger than predicted.

2. Experimental Apparatus and Method

Figure 3 shows the schematic diagram of the experimental apparatus, which consists of a flow entry section, a heat transfer test setion, an orifice flow meter, a blower with a controllable DC motor, a power supplier and data acquisition systems. A bell-mouth entry section and downstream section of the main test part were made up of nominal 4.4 cm arcylic pipe. The core of the experimental apparatus consisted of a microchannel heat sink and a manifold shown in Fig. 4,

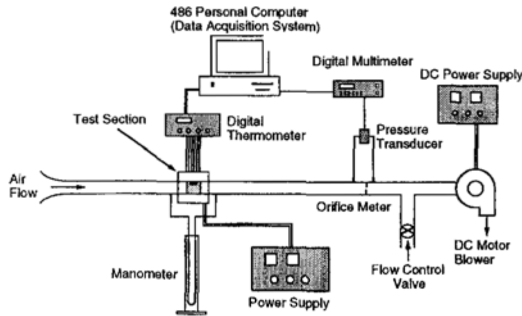

Fig. 3 Schematic diagram of an experimental apparatus.

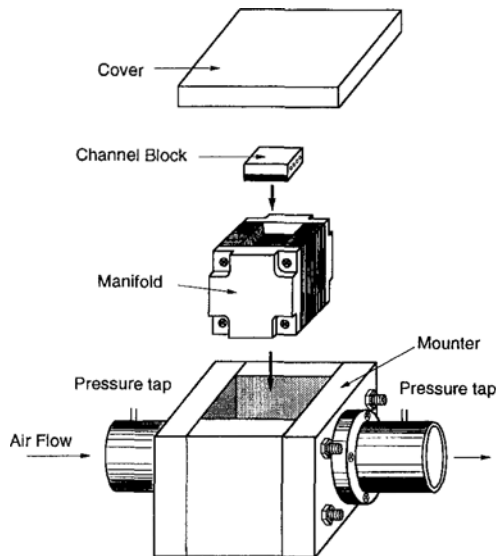

Fig. 4 Disassembled configuration of a main test section.

which was enclosed again by a 3-cm-thick acrylic cube for insulation and sealing up. Additionally, the main test part was wrapped with a 3 cm thick fiberglass blanket to minimize the parasitic heat loss. Two wall pressure taps were made to measure the differential pressure drops across the manifold microchannel, where they were located at the 1.5 diameter away from both edges of a sealing box.

Microchannel heat sinks were fabricated by a CNC wire cutting machine from an oxygen-free copper block (30 mm$\times$30.8 mm$\times$15 mm). Four cartridge heaters (1/8″ in diameter and maximum power of 25W for each) were inserted symmetrically on the opposite side of the machined micro-

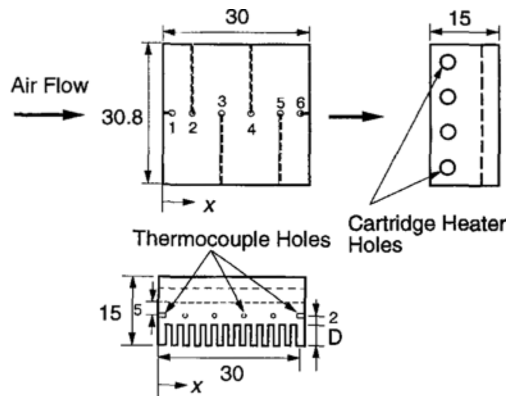

Fig. 5 Detailed view of a microchannel heat sink and thermocouple locations.

channels to establish a uniform heat flux boundary condition at the microchannel base. The heater module temperature was determined from six T-type thermocouples positioned 2.0 mm below the microchannel base at the centerline along the flow direction. Those thermocouples on the interior of the module were inserted in blind holes drilled just large enough to accomodate the 32 gage thermocouples wires and insulation. Figure 5 shows the detailed feature of a microchannel heat sink and thermocouple locations trigonometrically. The actual microchannel base temperature was determined from these measurements made below the surface using a one-dimensional Fourier conduction approximation. In addition to the surface temperature correction there was non-negligible temperature variation of the microchannel base along the flow direction due to the different impinging effect of coolant flowing into the microchannel from the manifold. However, the maximum temperature difference on the module, in all experiments, was below 0.4℃ since it was made of highly conductive material. The average microchannel base temperature, $\overline{T}_s$, was then determined from an area average of this temperature variation. The total heat transfer, Q, was determined from the electrical dissipation in the cartridge heaters, which was calculated from the Ohm's law using voltage and current measurements recorded at each test run. The parasitic heat losses to the surroundings were estimated from an one-dimensional Fourier conduction law and

found to be negligible. These were also assured by comparing the heat dissipations with temperature rises of coolant, whose the maximum deviation was within 3% in all the experiments.

A total of 9 diffeent microchannel heat sinks were fabricated in order to investigate the effects of the geometrical parameters in manifold microchannel heat sinks. Table 1 lists the detailed dimensions of microchannels used in the present experiments. Here δ_c, D and δ_w are microchannel width, microchannel depth and fin thickness, respectively.

The manifold consists of an assembly of acrylic plates, held together by four bolts, one in each

Table 1 Detailed dimension of microhannels used. [unit : mm]

No.	σ_c	σ_ω	D	σ_ω/σ_c
1	0.35	0.44	5.35	1.26
2	0.55	0.44	5.34	0.82
3	1.00	0.44	5.15	0.43
4	0.82	0.62	5.25	0.76
5	0.62	0.82	5.20	1.32
6	0.38	1.06	5.34	2.79
7	0.43	1.00	5.34	2.33
8	0.43	1.00	2.57	2.33
9	0.43	1.00	10.56	2.33

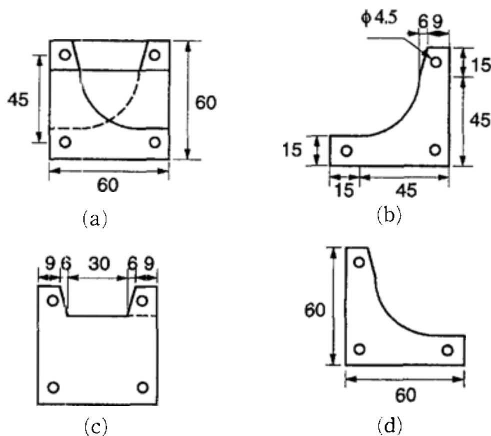

Fig. 6 Construction of manifold : (a) end, (b) inlet, (c) flow divider, and (d) outlet.

corner. Figure 6 shows the parts of the manifold prior to assembling. All the pieces were machined by a CNC milling machine with acrylic plates. The inlet and outlet pieces with an equal wall -thickness were identical but reversed. An additional acrylic piece was attached to the one side top of a flow divider (see a dashed line in Fig. 6 (c)) to provide an equal thickness to the cut parts of an inlet and an outlet in machining process. The end pieces were machined with 15 mm thick acrylic blocks. When assembled, the acrylic plates and end pieces form a 60 mm cube with a 42 mm tapered square opening. Two different sizes of manifold were made in order to examine the effect of the geometric parameters of manifold. Table 2 shows the detailed dimensions for each manifold. As shown in the table, manifold 2 has wider inlet/outlet channel widths compared with those of manifold 1, which result in the increase of manifold inlet/outlet channel number. Of note is that an additional manifold having one inlet channel and one outlet channel was fabricated so that the experiments for the traditional microchannel heat sinks could be performed.

The orifice meter was used to measure the volume flow rate. The normal type orifice plate with an aspect ratio of 0.4 and D and $D/2$ tapping was adopted. Prior to the experiments, the orifice meter was calibrated with the standard measurement system installed in Korea Research Institute of Standards and Science and also connected to the main test section according to the regulation of ISO 5167-1 (1991). The volume

Table 2 Detailed dimension of Manifolds used. [unit : mm]

	Manifold 1	Manifold 2
Inlet		
No.	3	8
Width (t)	4.0	0.9
Flow divider		
No.	6	16
Thickness (t^*)	0.9	0.9
Outlet		
No.	4	9
Width (t)	4.0	0.9

flow rate was controlled by a variable DC motor attached to a blower and a by-pass valve. All the data of temperature, pressure, flow rate and dissipated power during the experiments were recorded and plotted by the data aquisition system (*Data Translation, U. S. A.*) installed in a personal computer.

In general the thermal performance of a heat sink is characterized by its thermal resistance defined as $\Theta=(\overline{T}_s-T_i)/Q$, where $(\overline{T}_s-T_i)$ presents the difference between the average microchannel base temperature and the inlet temperature of coolant and Q the dissipated power, respectively.

3. Results and Discussion

The experimental data representing the effects of various geometrical parameters were collected and analyzed. The results were shown in the thermal resistance vs. the pumping power. The pumping power is the product of the volume flow rate and the pressure drop through a manifold microchannel heat sink.

Figure 7 shows the effect of the microchannel width on the thermal performances of manifold microchanel heat sinks. The microchannels have the same fin thickness and almost the same channel depth, but different channel width. Fig. 7(a) presents the thermal resistances of microchannel heat sinks with manifold 1 having the manifold inlet/outlet channel width of 4 mm. As expected, the thermal resistances of heat sinks were significantly reduced with increasing the pumping power regardless of the microchannel width. The thermal resistances were also reduced as the microchannel width decreased. It might be primarily due to the increase of heat transfer surface area in microchannels since the larger number of microchannel could be fabricated on the finite size of a heat sink as the microchannel width was reduced.

Also, the thermal resistance of the narrow channel ($\delta_c=0.35$ mm) was slightly more dependent on the pumping power than that of the wide channel ($\delta_c=1.00$ mm). It could be explained by the occurrence of impinging effect at the heat sink

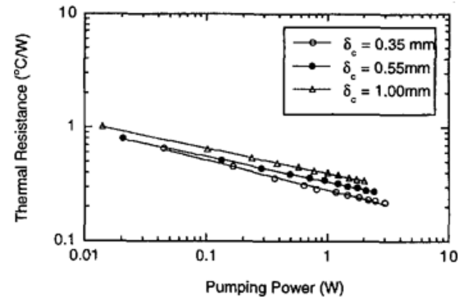

(a) MMC (Manifold 1)

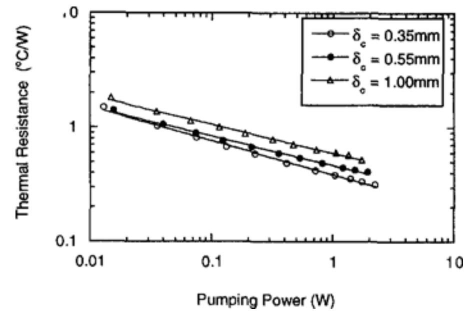

(b) MMC (Manifold 2)

Fig. 7 Effect of microchannel width δ_c ($\delta_w=0.44$ mm, $D=5.15-5.35$ mm).

surface area, whether normal to the jet (the microchannel floor and top of the walls) or planar (the sides of the microchannel walls). Figure 7(b) presents the themal resistances of the microchannel heat sinks with manifold 2 having manifold inlet/outlet channel width of 0.9 mm. Similar trend was shown in Fig. 7(a). However, when compared with Fig. 7(a) the thermal resistances of microchannel heat sinks increased significantly, i. e., approximately 2 times, with decreasing manifold inlet/outlet channel width. The reason could be summaried as follows :

Figure 8 shows the cross-setional view of the 'unit cell' of the symmetric flow domain in a maifold microchannel heat sink. In case of manifold 1, since the ratio of the microchannel depth to the manifold channel width (D/t) is approximately 1.3, the flow configuration can be considered as the flow through the 180° bent rectangular channel without abrupt change of flow area through the manifold microchannel. On the other hand, microchannel flow through manifold 2 seems to be the flow with abrupt change of the

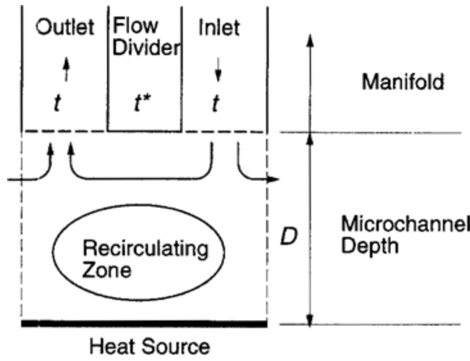

Fig. 8 Flow behavior in the 'unit cell' of a MMC heat sink with high D/t.

flow area since the D/t is quite larger than unity, i. e., 5.9. As a result, the recirculation zone may be formed at the bottom of microchannel since the large amount of fluid bypasses through only the top side of microchannel. However, the flow velocity in the microchannels increases since the sum of flow inlet areas decreases with decreasing the manifold inlet/outlet channel width. This combined effects were shown in Fig. 7, which resulted in reduction of the thermal performances of manifold microchannel heat sinks. Similar trends to the effects of manifold were shown throughout the remaining results of the present study.

Figures 9(a) and 9(b) present the effects of the thickness-width ratio on the thermal resistances of microchannel heat sinks with manifold 1 and manifold 2, respectively. The thickness-width ratio was defined as the ratio of fin thickness to the microchannel width and the microchannel depth was fixed at 5.15~5.34 mm. In this case, since the sum of the microchannel width and the fin thickness were fixed with 1.43~1.44 mm, there was the same number of microchannels on the confined size of a heat sink, which implied the heat transfer surface areas were almost the same. However, the total flow cross-sectional area of microchannels decreased with increasing the thickness-width ratio. It also caused to the increase of the thermal resistance and the pressure drop of heat sinks. The results of these combined effects were shown in Fig. 9. In general, the thermal resistance of heat sinks was more or less

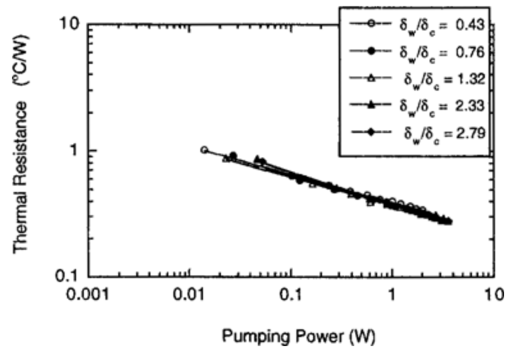

(a) MMC (Manifold 1)

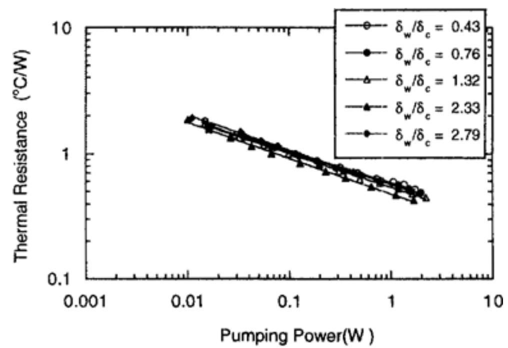

(b) MMC (Manifold 2)

Fig. 9 Effect of the thickness-width ratio, δ_w/δ_c ($\delta_w + \delta_c$ = 1.43~1.44 mm, D=5.15~5.34 mm).

weater dependent on the thickness-width ratio than the microchannel width. Also, the thermal resistance of heat sinks decreased as the thickness-width ratio increased. However, it was found that there existed the optimum thickness-width ratio of 2.33 in the range of the present experiments, which was seen more clearly in case of manifold 2 (see Fig. 9(b)).

The effects of the microchannel depth on the thermal perfermance of manifold micrchannel heat sinks are shown in Fig. 10. The dimensionless thickness-width ratio was fixed at 2.33 as optimum. As seen in the figure, the thermal resistance was reduced as the channel depth increased. However, it was not reduced further at larger microchannel depth than 5.34 mm under the present experimental range, which might be attributed to loss of fin efficiency. As seen in Fig. 9(b), the effect of the microchannel depth was getting weak as the manifold channel number

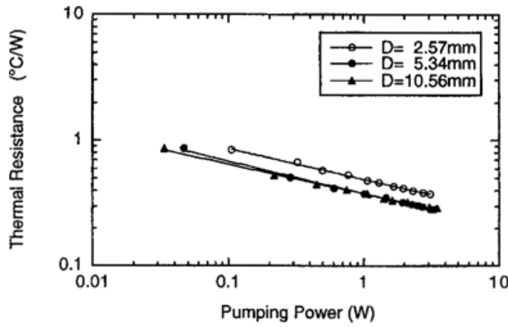

(a) MMC (Manifold 1)

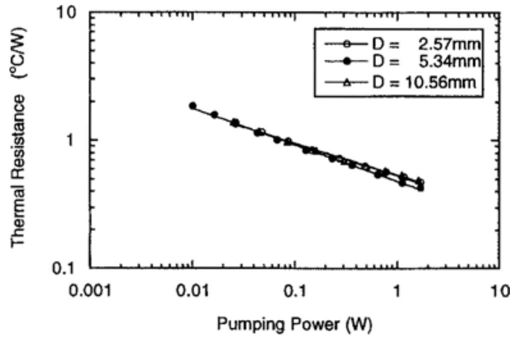

(b) MMC (Manifold 2)

Fig. 10 Effect of microchannel depth. $D(\delta_w/\delta_c=2.33)$.

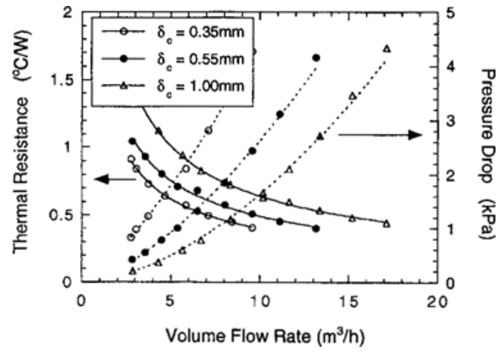

(a) TMC

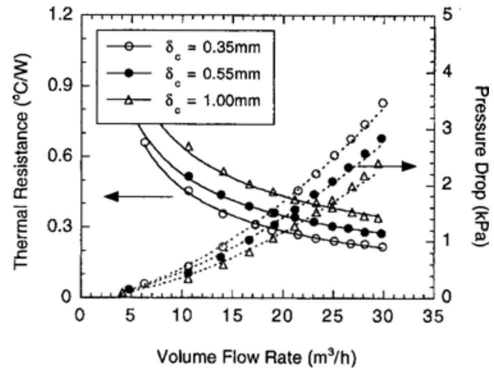

(b) MMC (Manifold 1)

Fig. 11 Comparison of the thermal resistance and pressure drop of the MMC heat sinks with those of the TMC heat sinks.

increased, which could be explained by the formation of the recirculation zone at the bottom of microchannel as aforementioned. Also, the thermal resistances of the manifold microchannel heat sinks increased with the number of manifold channel due to the same reason.

So far, the experimental results have presented only the geometrical effects of the manifold microchannel heat sinks, which have not indicated any advantages of using a manifold in microchannel heat sinks. As mentioned earlier, the microchannel heat sink without a manifold was termed as traditional microchannel (TMC) while the microchannel heat sink with a manifold as manifold microchannel (MMC). Representative performance comparison of those two heat sinks was shown in Fig. 11. Unlikely to the previous figures, the results were presented as the thermal resistances and pressure drops verse the volume flow rate. When the hydrodynamic and thermal performances were compared at a given volume flow rate, the thermal resistances of MMC heat sinks with manifold 1 were slightly lower than those of TMC heat sinks while the corresponding pressure drops were significantly lower. It might be primarily attributed to the decrease of flow velocity in the microchannels since the coolant was split by many manifold inlet channels. As mentioned earlier, the high pressure drop through a heat sink is one of crucial constraints in the application of microchannel to cool the multichip module. Conclusively, the pressure drops of the microchannel heat sinks could be reduced greatly without excessive heat transfer penalty by using a manifold.

Figure 12 shows the comparison of the thermal performance of those two heat sinks. In this case, the thickness-width ratio and the microchannel depth were fixed with 2.33 and 5.34 mm, respectively as optimum. As seen in the figure, the

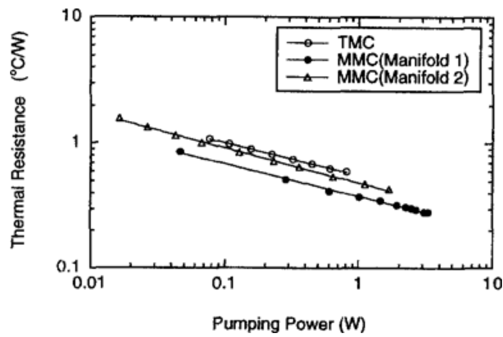

Fig. 12 Manifold effect on the thermal performance of the MMC heat sinks ($\delta_w/\delta_c=2.33$, $D=$ 5.34 mm).

thermal resistance of a MMC heat sink with Manifold 1 was reduced approximately up to 35% when compared with that of a TMC heat sink, which clearly demonstrates advantage of using a manifold in microchannel heat sinks.

4. Summary and Conclusions

An experimental investigation has been carried out to understand the effects of various geometrical parameters on the thermal performance of manifold microchannel heat sinks for the forced air cooling. Also, the thermal resistance of those heat sinks was compared with that of the traditional microchannel heat sinks to examine the effectiveness of using a manifold. Important findings are briefly summarized below.

1. The thermal resistance of manifold microchannel heat sinks was strongly effected by the pumping power, the microchannel width and the manifold inlet/outlet channel width, but weakly by the thickness-width ratio and the microchannel depth coorporated with the manifold inlet/outlet channel width. Especially, it was found that the ratio of the manifold channel width to the microchannel depth (D/t) was an importment parameter in the optimal design of the manifold microchannel heat sinks.

2. In general, the thermal resistance of heat sinks decreased as the microchannel depth and the thickness-width ratio increased. However, it was found that there existed the optimum values of those parameters, i. e., $\delta_w/\delta_c=2.33$ and $D=5.34$ mm, under the current experimental range.

3. Pressure drops of microchannel heat sinks could be reduced greatly by using a manifold without excessive heat transfer penalty. Under the optimum condition of geometrical parameters, the thermal resistance of MMC heat sink with manifold 1 at a fixed pumping power was approximately 35% lower than than that of TMC heat sink, which clearly demonstrated the effectiveness of using a manifold.

Acknowledgement

The authors acknowledge the financial support of the Korea Science & Engineering Foundation under its Grant No. 951-1007-061-2. In addition, the authors wish to express appreciation to Dr. David Copeland, manager of thermal engineering at Intricast Co., Inc., U. S. A., for useful discussions.

References

Goldberg, N., 1984, "Narrow Channel Forced Air Heat Sink," *IEEE Trans. on Components, Hybrids, and Manufacturing Technology*, Vol. 7, No. 1, pp. 154~159.

Gromoll, B., 1994, "Advanced Micro Air-cooling Systems for High Density Packaging," *Proc. IEEE SEMI-THERMTM Symposium*, pp. 53~58.

Harpole, G. M., and Eninger, J. E., 1991, "Micro-Channel Heat Exchanger Optimization," *Proc. of the 7th IEEE Semi-Therm Symp.* pp. 59~63.

ISO 5167-1, 1991, "Measurement of Fluid Flow by Means of Differential Pressure Devices," International Standards Organization.

Kleiner, M. B., Kuhn, S. A. and Haberger, K, 1995, "High Performance Forced Air Cooling Scheme Employing Microchannel Heat Exchangers," *IEEE Transactions on Components, Packaging, and Manufacturing Technology-Part A*, Vol. 18, No. 4, pp. 795~804.

Knight, R. W., Goodling, J. S., and Hall D. J., 1991, "Optimal Thermal Design of Forced Convection Heat Sinks-Anaylitical," *ASME Trans.,*

J. of Electronic Packaging, Vol. 113, pp. 313 ~321.

Knight, R. W., Hall, D. J., Goodling, J. S. and Jaeger, R. C., 1992a, "Heat Sink Optimization with Application to Microchannels," *IEEE Trans. on Components, and Manufacturing Tech.*, Vol. CHMT-15, No. 5, pp. 832~842.

Knight, R. W., Goodling, J. S., and Gross, B. E., 1992b, "Optimal Thermal Design of Air Cooled Forced Convection Finned Heat Sinks -Experimental Verification," *IEEE Trans. on Components, Hybrids, and Manufacturing Technology*, Vol. 15, No. 5, pp. 754~760.

Pak, B. C., Copeland, D. and Nakayama, W., 1995, "Cooling of Electronic Systems by Using Manifold Microchannel Heat Sinks," *Proc. of the KSME Fall Annual Meetings '95*, Vol. Ⅱ, Vol. 3, pp. 74~80.

Phillips, R. J., 1990, "Microchannel Heat Sinks," *in Advances in Thermal Modeling of Electronic Components and Systems*, Vol. 3, ASME Press.

Schulenberg, N., Kvamme, E., Nelson, A., Roh, J, Phillips, J. R., Mansingh, V., and Blackman, J., 1989, "Evaluation of Air-cooled Microchannel Heat Sinks," *Proc. of the 9th Int. Electronics Packaging Conference*, pp. 913~924.

Tuckerman, D. B., and Pease, R. F. W., 1981, "High-Performance Heat Sinking for VLSI," *IEEE Electron Device Letters*, Vol. 2, No. 5, pp. 126~129.

Yu, S. -P., and Xin, M. -D., 1994, "Analysis and Experiment on Gas Convection Microchannel Heat Exchangers," *Proc. of the 10th International Heat Transfer Conference*, Vol. 4, pp. 459 ~464.